

Fine-grained Private Knowledge Distillation

Shaowei Wang¹, Yuntong Li¹, Yingying Wang¹, Jin Li¹
Yuqiu Qian², Bangzhou Xin³, Wei Yang³

¹ Institute of Artificial Intelligence and Blockchain, Guangzhou University, Guangzhou, China.

² Interactive Entertainment Group, Tencent Games, Shenzhen, China.

³ Institute of Advanced Research, University of Science and Technology of China, Suzhou, China.

Abstract

Knowledge distillation has emerged as a scalable and effective way for privacy-preserving machine learning. One remaining drawback is that it consumes privacy in a model-level (i.e., client-level) manner, every distillation query incurs privacy loss of one client’s all records. In order to attain fine-grained privacy accountant and improve utility, this work proposes a model-free *reverse k -NN labeling* method towards record-level private knowledge distillation, where each record is employed for labeling at most k queries. Theoretically, we provide bounds of labeling error rate under the centralized/local/shuffle model of differential privacy (w.r.t. the number of records per query, privacy budgets). Experimentally, we demonstrate that it achieves new state-of-the-art accuracy with one order of magnitude lower of privacy loss. Specifically, on the CIFAR-10 dataset, it reaches 82.1% test accuracy with centralized privacy budget 1.0; on the MNIST/SVHN dataset, it reaches 99.1%/95.6% accuracy respectively with budget 0.1. It is the first time deep learning with differential privacy achieve comparable accuracy with reasonable data privacy protection (i.e., $\exp(\epsilon) \leq 1.5$). Our code is available at <https://github.com/liyuntong9/rknn>.

Introduction

Federated machine learning benefits from data across multiple individuals or organizations. However, data privacy has been a critical issue during collaboration, especially under increasingly rigid privacy laws, such as General Data Protection Regulation in the Europe Union, California Consumer Privacy Acts in California, and Data Security Law of the PRC in China. In contrast to transmitting raw data among clients, the seminal work of federated learning (Konečný et al. 2016) proposes to share gradients. Subsequent works (Wei et al. 2020; Luo et al. 2021) further impose rigorous protections (e.g., differential privacy (Dwork 2006)) on the gradients. Since iteratively transmitting gradients is inefficient (especially for deep neural networks), researchers (Papernot et al. 2016, 2018) begin to employ the paradigm of knowledge distillation (Hinton, Vinyals, and Dean 2015). Federation clients are asked to label public-available data with locally-trained models (see the top of Figure 1), meanwhile preserving the privacy of clients’ local records. Because labels have much lower dimensionality than gradients, federated knowledge distillation has become a communication&privacy efficient and thus prevalent way to federated

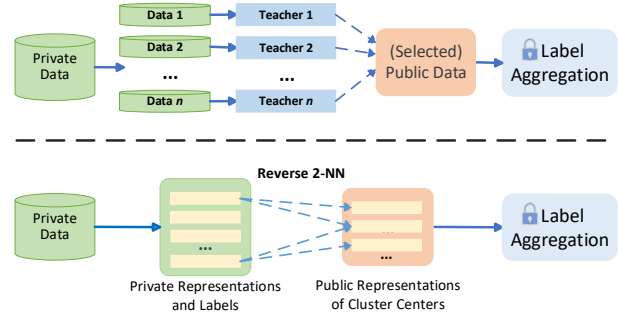


Figure 1: Comparison of the current paradigm of federated knowledge distillation (top) and our record-level private knowledge distillation with reverse k -NN (bottom).

deep learning (Lyu and Chen 2020; Zhu, Hong, and Zhou 2021).

Despite many advantages over sharing gradients, the current knowledge distillation paradigm is still suffering from a critical drawback on privacy accountant. Instead of accounting privacy loss at the record level as the gradient-sharing paradigm, one client’s records in the knowledge-distillation paradigm are summarized to a privacy-sensitive local model. When answering a distillation query with the local model, it is then almost intractable to account for each record’s contribution to the answer, or to concisely derive each record’s privacy loss.

Such a coarse client-level privacy consumption wastes privacy budget and fails to extract maximum knowledge from each record. Therefore, this work initializes the study of federated knowledge distillation with record-level (pure) differential privacy. With the help of unsupervised representation learning, we propose the model-free *reverse k -NN labeling* to achieve bounded contribution and constant privacy loss of every record. As demonstrated in Figure 1, every record is associated with k nearest neighboring querying samples, hence its privacy loss scales with only k instead of the number of total queries. In concise, the advantages of this novel method over the current paradigm of federated knowledge distillation are two-fold:

- **Fine-grained privacy accountant.** As opposed to the current paradigm that every record’s contribution and pri-

privacy loss (through local model) can not be separately accounted for, the new method limits one single record’s contribution, which enables more fine-grained privacy accountants and better knowledge elicitation.

- **Broad application scenarios.** Instead of relying on a locally trained model that needs hundreds of training records, our method only needs an appropriate distance measure (e.g., via learned representations) for reverse k -NN. Therefore, it could apply to both the cross-silo (i.e., every client has relatively abundant records) and cross-device (i.e., every client has only a few records or one record) settings in federated learning. Besides, it is naturally immune to data *Non-I.I.D.* settings and incurs only few-rounds communication.

Contributions

This work formulates the model-free reverse k -NN labeling problem as *Bucketized Sparse Vector Summation*, and then provides thorough solutions for the problem under centralized/local/shuffle differential privacy (Dwork 2006). Theoretically, We also analyze the labeling error rate of proposed solutions. The contributions of this paper are as follows.

- We initialize the study of federated knowledge distillation with record-level privacy preservation, and propose the model-free reverse k -NN query labeling method for achieving record-level (pure) differential privacy.
- We formulate the model-free reverse k -NN labeling problem as Bucketized Sparse Vector Summation (i.e., BSVS), and provide concrete mechanisms & theoretical guarantees for the problem under centralized/local/shuffle differential privacy.
- For the first time, we show that the most stringent scenario of local private federated deep learning (with knowledge distillation) is practical. It reaches 98.5% test accuracy on MNIST and 78.2% test accuracy on CIFAR-10 with a reasonable local budget $\epsilon = 0.4$.
- Through experiments, we demonstrate that our method achieves a significant accuracy boost meanwhile consuming an order of magnitude less of privacy budget when compared to existing approaches.

Related Work

We here retrospect efforts toward private and accurate knowledge distillation. The seminal work of knowledge distillation (Hinton, Vinyals, and Dean 2015) transfers knowledge from a large teacher model to a compact student model, aims for boosting inference efficiency and accuracy simultaneously. Nowadays researches on decentralized/federated learning (Papernot et al. 2016, 2018; Lin et al. 2020) employ ensemble knowledge distillation as a communication&privacy efficient learning paradigm beyond gradient/parameter aggregation (Abadi et al. 2016).

Some studies (e.g., in (Sun and Lyu 2020)) discover that knowledge distillation naturally resists membership inference attacks to some extent. For formally guaranteeing data privacy, it is necessary to conform to the centralized/local/shuffle differential privacy (DP) during distilla-

tion. Specifically, one line of studies inject Laplace/Gaussian random noise for preserving centralized ϵ -DP on aggregated labels (Papernot et al. 2018; Wang et al. 2019) from teacher models; another line of studies firstly sanitize the teacher model’s label locally (Sun and Lyu 2020; Lyu and Chen 2020), and then aggregate these local ϵ -DP labels. Recently, for bridging the advantages of centralized DP (i.e., high accuracy) and local DP (i.e., minimum trust), several studies (Liu et al. 2020; Feldman, McMillan, and Talwar 2021) propose shuffling messages from clients.

Note that all these studies consider client-level DP preservation, because of the impossibility to bound the worst-case contribution of one record in the teacher model. The most closely related works (Zhu et al. 2020a,b) try to account for one single record’s contribution when distilling knowledge with k -NN. However, to work around the worst-case contribution in k -NN (see Section), they only guarantee an approximate&data-dependent version of DP. In contrast, our work realizes rigorous pure DP accountant at the record level and achieves significant accuracy improvements.

Preliminaries

Federated Knowledge Distillation

Every data record (x, y) is sampled from a Cartesian domain $\mathcal{X} \times \mathcal{Y}$, where the sample x might be a tabular vector, an image, and etc. The class label y can be a binary value (i.e. $\mathcal{Y} = \{0, 1\}$) or categorical value (e.g., $\mathcal{Y} = \{0, 1, \dots, 9\}$ in hand-written digit recognition). Assume that the client i possesses m_i records, we let D^i denote these records as $D^i = [(x_1^i, y_1^i), \dots, (x_{m_i}^i, y_{m_i}^i)]$, and let D_{priv} denote the union of all local datasets:

$$D_{priv} = \bigcup_{i=1}^n D^i.$$

Let $D_{pub} = [(x_1, ?), \dots, (x_{m_{pub}}, ?)]$ denote the public unlabeled dataset possessed by the federation orchestrator, the primary goal of federated knowledge distillation/transfer is then labeling D_{pub} with knowledge from the D_{priv} . Current approaches (Papernot et al. 2018; Li and Wang 2019; Lyu and Chen 2020) are utilizing proxy models (e.g., neural networks) for answering labeling queries (every model is locally trained on D^i).

Centralized Differential Privacy

For datasets D_{priv}, D'_{priv} that are of the same size and differ only in *one record*, they are called *neighboring datasets*. The centralized DP (Dwork 2006) at record-level with budget (ϵ, δ) is as follows. As comparison, the client-level DP corresponds to neighboring datasets differ at one client’s data.

Definition 1 (Centralized (ϵ, δ) -DP). *Let \mathcal{K} denote the output domain, a randomized mechanism K satisfies ϵ -differential privacy iff for any neighboring datasets D, D' , and any outputs $\mathbf{z} \subseteq \mathcal{K}$,*

$$\mathbb{P}[K(D) \in \mathbf{z}] \leq \exp(\epsilon) \cdot \mathbb{P}[K(D') \in \mathbf{z}] + \delta.$$

Local Differential Privacy

Let K denote a randomized mechanism for sanitizing a single record, the local DP (Duchi, Jordan, and Wainwright 2013) is as follows.

Definition 2 (Local ϵ -DP). *Assuming each client holds a dataset D with only one record, a randomized mechanism K satisfies local ϵ -differential privacy iff for any data pair $D, D' \in \mathcal{X} \times \mathcal{Y}$, and any output $z \in \mathcal{K}$,*

$$\mathbb{P}[K(D) = z] \leq \exp(\epsilon) \cdot \mathbb{P}[K(D') = z].$$

Shuffle Differential Privacy

As a remedy to the low utility issue of the local privacy model, researchers (Bittau et al. 2017) propose the shuffle privacy model, where semi-trusted shufflers (or anonymous channels) lie between clients and the server. Let K denote the local randomizer, and $t^i = K(D^i)$ denote the private message(s) from the client i , the definition of shuffle (ϵ, δ) -DP is as follows.

Definition 3 (Shuffle (ϵ, δ) -DP). *The randomized mechanism K satisfies shuffle (ϵ, δ) -differential privacy iff the unordered union set $\bigcup_{i=1}^n t^i$ satisfies centralized (ϵ, δ) -DP constraints for the dataset D_{priv} .*

Reverse k -NN Labeling for KD

We now introduce the reverse k -NN labeling method for federated knowledge distillation. To clarify its principles of design, we compare it with the conventional k -NN. Without loss of generality, we here consider image classification and it can be applied to other domain (e.g., tabular data, natural language, video, etc.) without much effort.

Methodology

In the reverse k -nearest-neighbors labeling, for limiting every private record’s contribution, each record is associated with at most k (nearest) query samples; in order to improve the labeling accuracy, learned representations (instead of raw pixels) are utilized for distance measurement. At each learning iteration (see Algorithm 1), the method follows four steps.

Learning to Represent: Since raw pixels are unstable w.r.t. semantic labels, we measure sample distance by their latent representations. One can use pre-trained representation models (e.g., vision Transformers), or train an unsupervised representation model from scratch (e.g., via self-supervised learning (Chen et al. 2020)) with public-available D_{pub} .

Selecting Queries: Labeling all samples in D_{pub} is communication/computation/privacy expensive. Follow current approaches (Papernot et al. 2018; Wang et al. 2019), we select representative samples from D_{pub} . At the first iteration, we cluster D_{pub} into s groups in the representation space, and treat cluster centers $Q = [q_1, q_2, \dots, q_s]$ as query samples. For later iterations, samples are selected adaptively w.r.t. uncertainty of the current model M_S .

Algorithm 1: Record-level private KD

Input: n clients, private datasets $\mathcal{D}^1, \dots, \mathcal{D}^n$, unlabeled public dataset \mathcal{D}_{pub} .

Parameter: number of iterations T , number of nearest neighbors k , number of query samples s , privacy budget ϵ .

Output: student model M_S satisfies ϵ -differential privacy.

```

1: for  $t=1,2,\dots,T$  do
2:   select  $s$  query samples  $\mathcal{D}_{query}$  from  $\mathcal{D}_{pub}$ 
3:   // Client side
4:   for  $i=1,2,\dots,n$  do
5:     connect each local record  $(x_j^i, y_j^i) \in \mathcal{D}^i$  to  $k$ -nearest queries in  $\mathcal{D}_{query}$ 
6:     find  $k$ -nearest neighbors  $N_j^i \subseteq [1 : s]$  of  $x_j^i$ 
7:     represent the labeling answer on each query  $l \in [1 : s]$  as  $a_l^i = \sum_{l \in N_j^i} y_j^i \in \mathbb{R}^{|\mathcal{Y}|}$ 
8:     send all labeling answers  $A^i = [a_1^i, a_2^i, \dots, a_s^i]$ 
9:   end for
10:  // Server side
11:  aggregate the label counts  $a_l = \sum_{i=1}^n a_l^i \in \mathbb{R}^{|\mathcal{Y}|}$  from all clients for each  $l \in [1 : s]$ 
12:  ensemble  $A = [a_1, a_2, \dots, a_s]$  and add noise to  $A$  by  $\epsilon$ -differential privacy
13:  derive labels  $\{\hat{y}_l\}_{l=1}^s$  from noisy counts  $A$ 
14:  train student model  $M_S$  on  $\mathcal{D}_{query}$  with labels  $\{\hat{y}_l\}_{l=1}^s$ 
15: end for
16: return  $M_S$ 

```

Local Labeling: Given queries $Q = [q_1, q_2, \dots, q_s]$, the client i connects these query samples with local records under the reverse k -NN rule. Every local record (x_j^i, y_j^i) is connected to k nearest query samples (in the representation space). Assume that the label y_j^i is presented in the one-hot vector form, and let $N_j^i \subseteq [1 : s]$ denote the set of query indices that are k nearest neighbors of x_j^i , then the labeling answer from client i is $A^i = [a_1^i, a_2^i, \dots, a_s^i]$, where $a_l^i = \sum_{j=1}^{m_i} \mathbb{1}[l \in N_j^i] y_j^i$.

Label Aggregation: Given the labeling answers A^1, \dots, A^n from clients, we summarize them as $A = [a_1, a_2, \dots, a_s]$, where $a_l = \sum_{i=1}^m a_l^i$. The final hard labeling results is then $(q_1, \hat{y}_1), \dots, (q_s, \hat{y}_s)$, where for $l \in [1 : s]$:

$$\hat{y}_l = \arg \max_{c=1}^{|\mathcal{Y}|} a_l(c).$$

The final soft labeling results are $(q_1, \bar{y}_1), \dots, (q_s, \bar{y}_s)$, where $\bar{y}_l = \frac{a_l}{\sum_{c=1}^{|\mathcal{Y}|} a_l(c)}$. After assigning every sample in D_{pub} with the label of its cluster center, a student model is built upon labeled \mathcal{D}_{pub} (iteration 1) or \mathcal{D}_{query} (iterations $[2 : T]$) with conventional cross-entropy loss.

The proposed method is highly efficient, the computational/communication cost of the client i is linear to number of local samples $|D^i|$ and queries s (i.e., $O(|D^i| \cdot s \cdot T + s \cdot |\mathcal{Y}| \cdot T)$ and $O(s \cdot |\mathcal{Y}| \cdot T)$). Compared to the classical knowledge

distillation paradigm, it has the advantage of avoiding local model training, thus fits both resource-rich cross-silo and resource-scarce cross-device settings.

Note that the summarized labeling answer A is independent from how private samples D_{priv} distribute among clients, and only depends on the whole D_{priv} . Therefore, the above method resists non-IID settings.

k -NN vs. Reverse k -NN

To tell apart our record-level approach from the current model-level paradigm for federated knowledge distillation, we here compare the reverse k -NN with k -NN labeling.

When the k -NN classifier works as a local model for labeling (e.g., in (Zhu et al. 2020a,b)), each query sample is associated with at most k records. However, from a record's perspective, it might be associated with all s query samples, hence its maximum-possible contribution (i.e., the sensitivity in differential privacy) to the final answer A is $\Theta(s)$. As a comparison, one record's contribution in the reverse k -NN is bounded by $\Theta(k)$ and is much smaller than $\Theta(s)$. This difference in worst-case contribution causes dramatic gaps when seeking a privacy/utility trade-off.

Note that seeking other connection rules having the same privacy guarantee as reverse k -NN is also possible, please refer to Appendix C for detail.

Centralized Private Mechanisms

In this section, we reformulate the reverse k -NN labeling as the problem of Bucketized Sparse Vector Summation (BSVS), then present centralized DP mechanisms for the problem, and provide corresponding labeling error bounds.

Reformulation

The key steps in the reverse k -NN labeling can be abstracted as Bucketized Sparse Vector Summation (see Definition 4). Compared to the histogram summation and generalized bucketed vector summation (Chang et al. 2021), a critical difference is that the vector we consider is sparse, as the label y_j^i is one-hot (in multi-class classification) or multi-hot (in multi-label classification).

Definition 4 (Bucketized Sparse Vector Summation). *In the BSVS problem, each datum corresponds to a set $T_j \subseteq T$ of k buckets and a sparse vector $y_j \in \{0, 1\}^{|\mathcal{Y}|}$ and $|y_j| = r$. The goal is to determine, for a given $t \in T$, the vector sum of bucket t , which is $a_t := \sum_{j=1}^{\sum_{i=1:n} m_i} y_j \llbracket t \in T_j \rrbracket$. An approximate oracle \tilde{a} is said to be (η, β) -accurate at t if we have $|a_t - \tilde{a}_t|_{+\infty} < \eta$ with probability $1 - \beta$.*

In the above reformulation, the number of buckets is equal to the number of query samples: $|T| = s$. Note that in conventional multi-class classification, we have $r \equiv 1$.

Mechanism and Accuracy Guarantees

When centralized $(\epsilon, 0)$ -DP is imposed on the BSVS problem, we employ the classical Laplace mechanism for privacy preservation. Apparently, the sensitivity Δ is the maximum possible magnitude of $A^i = [a_1^i, a_2^i, \dots, a_s^i]$ (i.e., $2k \cdot r$). Therefore, we inject $Laplace(\frac{2k \cdot r}{\epsilon})$ to every element

of A . The corresponding accuracy guarantee is presented in Proposition 1, which is derived from the tail probability bound of the Laplace distribution.

Proposition 1. *There is an $(\frac{2k \cdot r \cdot \log(|\mathcal{Y}|/\beta)}{\epsilon}, \beta)$ -accurate centralized ϵ -DP algorithm for the BSVS problem.*

For the t -th query/bucket, define the (non-private) count gap between the true label $y^* \in [1 : |\mathcal{Y}|]$ and false labels as:

$$Gap_t = a_t(y^*) - \max_{c \in [1:|\mathcal{Y}|] \text{ and } c \neq y^*} a_t(c),$$

we then have the following conclusion on the private labeling accuracy w.r.t. the accuracy of the BSVS problem:

Remark 1. *If $Gap_t \geq 2\alpha$ and the private algorithm is (α, β) -accurate, then with probability $1 - \beta$, the estimated hard labeling result is accurate (equals to the true label y^*).*

Local Private Mechanisms

Consider the most stringent case of imposing local DP on every client who holds only one record (i.e., $m_i \equiv 1$), every client i now sanitizes the labeling answer $A^i = [a_1^i, a_2^i, \dots, a_s^i]$ independently. Note that this case also fits cases one client holds multiple records, if we sample one record or simply normalizing labeling answers A^i . Naively, we could also adopt the Laplace mechanism and add $Laplace(\frac{2 \cdot k \cdot r}{\epsilon})$ to every element in A^i . However, it is dominated by the randomized response mechanism (Duchi, Jordan, and Wainwright 2013), which randomly flips every binary value in A^i with probability $\frac{1}{e^{\epsilon/(2kr)} + 1}$. We show randomized response is $(O(\sqrt{\frac{nk^2 r^2 \log(|\mathcal{Y}|/\beta)}{\epsilon^2}}), \beta)$ -accurate (in Theorem 1).

Theorem 1. *The local ϵ -DP randomized response mechanism is an $(\frac{e^{\epsilon/(2kr)} + 1}{e^{\epsilon/(2kr)} - 1} \sqrt{3n \log(|\mathcal{Y}|/\beta)} / (e^{\epsilon/(2kr)} + 1), \beta)$ -accurate algorithm for the BSVS problem when $\epsilon = O(1)$.*

Proof. Recall that for a binary value b flipped with probability $\frac{1}{e^{\epsilon/(2kr)} + 1}$, the unbiased estimation given the observation b' is $\tilde{b} = \frac{b' - 1 / (e^{\epsilon/(2kr)} + 1)}{(e^{\epsilon/(2kr)} - 1) / (e^{\epsilon/(2kr)} + 1)}$. The total count of observed ones is a summation of n Bernoulli variables with a success rate of either $\frac{1}{e^{\epsilon/(2kr)} + 1}$ or $\frac{e^{\epsilon/(2kr)}}{e^{\epsilon/(2kr)} + 1}$. Let u denote the estimation bias of one element in \tilde{a}_t , we have $\mathbb{P}[|u| > \eta \cdot \frac{e^{\epsilon/(2kr)} + 1}{e^{\epsilon/(2kr)} - 1}] \leq \exp(-\frac{\eta^2 (e^{\epsilon/(2kr)} + 1)}{3n})$. Therefore, with probability of $1 - \beta$, we have $|a_t - \tilde{a}_t|_{+\infty} \leq \frac{e^{\epsilon/(2kr)} + 1}{e^{\epsilon/(2kr)} - 1} \sqrt{\frac{3n \log(|\mathcal{Y}|/\beta)}{e^{\epsilon/(2kr)} + 1}}$. \square

Due to budget splitting, the randomized response is suffering from the error rate of $\tilde{\Theta}(\frac{k \cdot r}{\epsilon})$. We can actually adopt an optimal sparse vector summation oracle (in the high privacy regime) (Wang et al. 2021) for the BSVS problem and achieve an error rate of $\tilde{\Theta}(\frac{\sqrt{k \cdot r}}{\epsilon})$ (see Appendix A and B).

Shuffle Private Mechanisms

When messages from users are anonymized & shuffled by anonymous channels or shufflers, the server only observes a multi-set about messages. Consequently, to achieve a certain

level of (centralized) differential privacy, every client can inject fewer noises in the local. According to the number of messages one client may publish, the shuffle privacy model can be categorized into the multi-message one (Ghazi et al. 2020) and the single-message one (Feldman, McMillan, and Talwar 2021).

Multi-message Shuffling

In the multi-message shuffle privacy model, the basic idea is to add noises to A in a distributed manner. For the categorical distribution estimation problem with dimension d , (Ghazi et al. 2020) proposes an (ϵ, δ) -DP protocol with an error equal to adding independent $Laplace(\frac{4}{\epsilon})$, and with expected messages of one user equal to $1 + O(\frac{d \log^2(1/\delta)}{\epsilon^2 n})$, each consisting $\lceil \log d \rceil + 1$ bits. In the protocol, the $Laplace(\frac{4}{\epsilon})$ is decomposed into $\Theta(n)$ negative binomial variables and added to every entry in A^i accordingly. Each message is an index in $[1 : d]$, which means plus one to the index. For the BSVS problem with (ϵ, δ) -DP, follow almost the same protocol in (Ghazi et al. 2020), the $Laplace(\frac{4kr}{\epsilon})$ can be added in a distributed manner with expected messages of one client equal to $kr + O(\frac{dk^2 r^2 \log^2(1/\delta)}{\epsilon^2 n})$, each consisting $\lceil \log d \rceil + 1$ bits. Plugging into the analyses on Laplace mechanism in Proposition 1, we conclude that it is $(\frac{4kr \log(|\mathcal{Y}|/\beta)}{\epsilon}, \beta)$ -accurate.

Single-message Shuffling

When each client is constrained to send only one message to the shuffler, the message must be local DP (Cheu et al. 2019), while the privacy in the central perspective is amplified. Recently, (Feldman, McMillan, and Talwar 2021) gives a tight privacy amplification bound for any local private mechanisms, shows n local ϵ -DP and shuffled messages satisfy centralized $(\log(1 + (\frac{8\sqrt{e^\epsilon \log(4/\delta)}}{\sqrt{n}} + \frac{8e^\epsilon}{n}) \frac{e^\epsilon - 1}{e^\epsilon + 1}), \delta)$ -DP when $\log(\frac{n}{16 \log(2/\delta)}) \geq \epsilon$. In return, when centralized privacy budget (ϵ, δ) is given, we can reversely derive the enlarged local budget, and provide corresponding accuracy guarantees with Theorem 1.

Experiments

To validate proposed record-level private mechanisms for federated learning, we conduct extensive experiments on real-world datasets to answer the following questions: (1) What is the effect of query selection on accuracy? (2) What is the effect of parameter k on accuracy? (3) What is the performance gap between our approach and SOTA methods?

The competitive approaches include SOTA private knowledge distillation methods by adding Laplace noise (LNMAX) or Gaussian noise (GNMAX) in (Papernot et al. 2016, 2018), private k -NN (Zhu et al. 2020a) and the noisy SGD methods in (Luo et al. 2021). Our approach is implemented with $(\epsilon, 0)$ -DP, while competitive approaches are implemented with $(\epsilon, 10^{-5})$ -DP. Notice that given the representation model trained on the D_{pub} and the labeled samples in D_{priv} , one may also simply train a prediction head with noisy SGD (Abadi et al. 2016) as the classifier. We denote

this straight-forward approach as *Layer-1 noisy SGD* (with one prediction layer) and *Layer-2 noisy SGD* (with two prediction layers). Both Layer-1 and Layer-2 noisy SGD train parameters with the size of few thousands, which is much smaller than the whole classifier’s, but is still much larger than the label domain size $|\mathcal{Y}|$.

Datasets and Networks

Three popular image datasets are employed for experiments: **MNIST**¹ that contains 70,000 gray-scale images of size 28×28 , has 10 categories; **SVHN**² that contains 630,420 digit images of size 32×32 and 10 categories; **CIFAR-10**³ that contains 60,000 images of size 32×32 and 10 categories.

Follow common settings in the literature, for the MNIST, we assume the public data D_{pub} is 5,000 samples from the test dataset, the remaining 5,000 test samples are used for evaluating the performance of the student classifier, and the training dataset is used as the private data D_{priv} ; for the SVHN, we assume the public data D_{pub} is $26k$ samples from the test dataset, the remaining $1k$ test samples are used for evaluating the performance of the student classifier, and the training dataset, together with the extended data, is used as the private data D_{priv} ; for the CIFAR-10, we assume the public data D_{pub} is 30,000 samples from the training set, the 1,000 samples from the test dataset are used for evaluation, and use other 29,000 samples as the private data D_{priv} . The experimental results of shuffle DP is omitted, since it is analogy to centralized or local DP.

For the MNIST dataset, the architecture of the student classifier is from (An et al. 2020), and the DTI (Monnier, Groueix, and Aubry 2020) is employed for general purpose representation & clustering on D_{pub} (denoted as **[general]**). For the SVHN dataset, the architecture of the student classifier is Mixmatch (Berthelot et al. 2019), and the histogram of oriented gradients(HOG) (Dalal and Triggs 2005) and k -means++ is employed for general purpose representation & clustering on the D_{pub} . For the CIFAR-10 dataset, the network architecture is DenseNet121, and the SimCLR (Chen et al. 2020) and k -means++ is used for representation learning & clustering on the D_{pub} .

Performance Metrics

Two accuracy indications are employed for measuring the performances, one is the accuracy of the private label answering (Acc_{pl}), the other is the test accuracy of the privately learned classifier (Acc_{pc}). As we use unsupervised clustering for query selection at iteration 1, here the Acc_{pl} is the number of public samples receiving correct labels divided by $|D_{pub}|$.

Varying Number of Clusters

The purity of clusters (w.r.t. class labels) upper bounds the Acc_{pl} . Increasing s can roughly increase purity, but reduce the number of local records associated with one query. We

¹<http://yann.lecun.com/exdb/mnist>

²<http://ufldl.stanford.edu/housenumbers>

³<https://www.cs.toronto.edu/~kriz/cifar.html>

here explore the appropriate number s . When s changes within a certain range, we present the experimental results Acc_{pc} in Figure 2 for MNIST (with $\epsilon = 0.1$), Figure 3 for SVHN (with $\epsilon = 0.1$), and Figure 4 for CIFAR-10 (with $\epsilon = 1$). For the more simple MNIST, the best number of clusters is around 40; while for the SVHN/CIFAR-10, the accuracy increases with s , since it has more diversity in one class. The (omitted) experimental results on labeling accuracy Acc_{pl} are always 0.5%-3.0% behind the Acc_{pc} , imply building the classifier could suppress labeling noises due to privacy preservation.

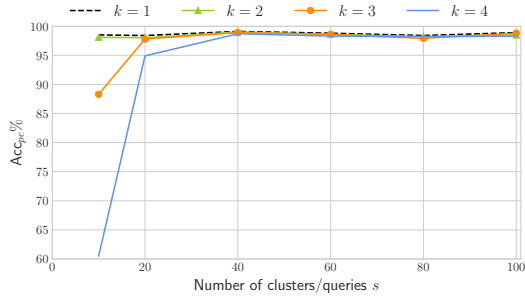


Figure 2: Experimental results on MNIST ($\epsilon = 0.1, T = 1$) with vary number of clusters s and vary number of neighbors k .

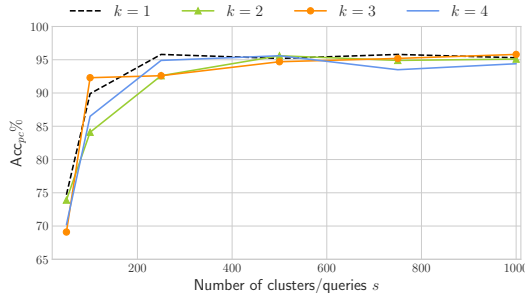


Figure 3: Experimental results on SVHN ($\epsilon = 1, T = 1$) with vary number of clusters s and vary number of neighbors k .

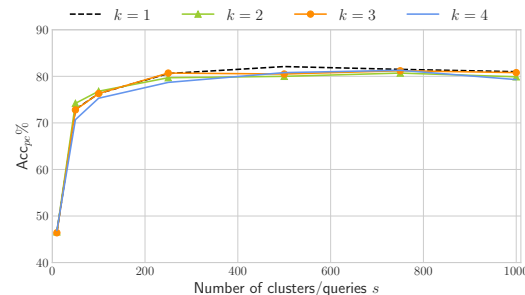


Figure 4: Experimental results on CIFAR-10 ($\epsilon = 1, T = 1$) with vary number of clusters s and vary number of neighbors k .

Varying k in Reverse Nearest Neighbors

We also explore the choice of k of reverse k -NN in Figures 2, 3, and 4. It is demonstrated that there is no noticeable

difference between choosing k at 1, 2, 3 or 4. Theoretically, as k gets larger, the label count of each query grows with k , but the count gap grows sublinear to k and the standard deviation of the privacy noise grows with k . Here the k in [1, 2, 3, 4] are all small, thus the sublinearity is negligible and the noises hardly overwhelm count gaps. It is experimentally observed that when k grows to about 10, the performances begin to drop significantly.

Local DP

For the most stringent case that local DP is imposed on every client's single record, we present results in Figure 5 for MNIST/CIFAR-10. Since noises due to local DP easily dominate Gap_t , we here fix hyper-parameters at $s = |\mathcal{Y}| = 10$ and $k = 1$, and employ end-to-end unsupervised clustering on MNIST with DTI (Monnier, Groueix, and Aubry 2020) and CIFAR-10 with SCAN (Van Gansbeke et al. 2020). It is observed that the Collision mechanism (Wang et al. 2021) achieves test accuracy of 98.5% for MNIST and 78.2% for CIFAR-10 with privacy budget $\epsilon = 0.4$. To the best of our knowledge, it is the first time local private deep learning provides meaningful privacy/accuracy trade-offs.

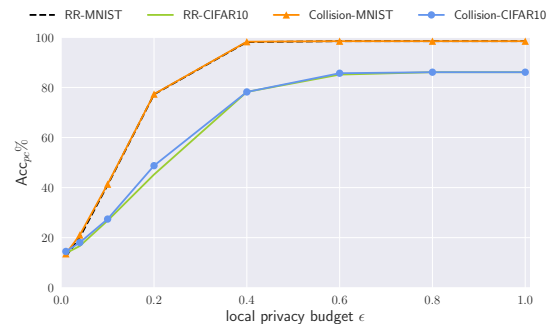


Figure 5: Local DP experimental results on MNIST/CIFAR-10 with randomized response (RR) and Collision mechanism (Collision), when ϵ ranges from 0.01 to 1.0.

Comparison with Existing Approaches

In Table 1, we compare our method's results with reported results of existing approaches with same settings. The hyper-parameter of our method is set to $T = 1$ and $k = 1$. When utilizing general purpose unsupervised representation learning and clustering, compared to existing client-level DP methods (i.e., LNMAX, GNMAX) or record-level approximate DP methods (i.e., Noisy SGD, Private k -NN), our method achieves better accuracy with an order magnitude smaller privacy consumption. Specifically, if we employ end-to-end unsupervised clustering (Monnier, Groueix, and Aubry 2020; Van Gansbeke et al. 2020) (denoted as [end2end]), we are able to achieve (average) accuracy of 86.1% with centralized $\epsilon = 0.01$ for CIFAR-10, and 99.1% accuracy for MNIST. When the number of query $s = |\mathcal{Y}|$, we have the count gap $\text{Gap}_t \approx |D_{priv}|/s$ is tens of hundreds, which is large enough to overcome Laplace noises with standard deviation $2\sqrt{2}/\epsilon = 2\sqrt{2}/0.01 < 300$.

Table 1: Test accuracy & privacy consumption comparison of centralized differentially private methods.

Dataset	Methods	#Queries	ϵ	Test Acc.	Label Acc.	Non-priv Acc.
MNIST	LNMAX (Papernot et al. 2018)	1000	8.03	98.1%		
	GNMAX (Papernot et al. 2018)	286	1.97	98.5%		99.2%
	Private k -NN (Zhu et al. 2020a)	735	0.47	98.8%		
	Noisy SGD (Abadi et al. 2016)		1.0	81.2%		91.1%
	Ours [general]	40	0.1	99.1%	98.5%	
	Ours [general]	40	0.04	98.6%	97.7%	99.2%
	Ours [end2end]	10	0.01	98.5%	97.5%	98.7%
SVHN	LNMAX (Papernot et al. 2018)	1000	8.19	90.1%		
	GNMAX (Papernot et al. 2018)	3098	4.96	91.6%		92.8%
	Private k -NN (Zhu et al. 2020a)	2939	0.49	91.6%		
	Noisy SGD (Abadi et al. 2016)		4.0	76.0%		84.4%
	Ours [general]	500	0.1	95.6%		96.7%
Ours [general]	500	0.04	95.3%			
CIFAR-10	GNMAX (Papernot et al. 2018)	286		< 50%		80.5%
	Private k -NN (Zhu et al. 2020a)	3877	2.92	70.8%		
	Finetuning Noisy SGD (Luo et al. 2021)		1.0	76.5%		
	Layer-1 Noisy SGD (Abadi et al. 2016)		4.0	73.7%		77.7%
	Layer-2 Noisy SGD (Abadi et al. 2016)		4.0	78.5%		80.9%
	Ours [general]	500	1.0	82.1%	77.1%	82.3%
	Ours [general]	500	0.29	79.4%	73.9%	
Ours [end2end]	10	0.01	86.1%	85.9%	86.2%	
Ours [end2end]	10	0.005	86.0%	85.7%		

Summary

In summary, our record-level private knowledge distillation method is an effective way to centralized/decentralized machine learning, and significantly outperforms the Private k -NN (Zhu et al. 2020a) that preserves only approximate& data-dependent record-level privacy. The 82.1% accuracy on CIFAR-10 also surpasses the SOTA accuracy 76.5% (with $\epsilon = 1$) of the noisy SGD method in (Luo et al. 2021), demonstrates the powerful privacy&utility trade-off of knowledge distillation with record-level privacy. When equipped with tighter privacy accountant by Rényi differential privacy for our approach (in future study) or when data is non-I.I.D. across clients, the performance gaps can be even larger.

Conclusion

This work tackled one major drawback remaining in federated learning with knowledge distillation, and advocated

for fine-grained record-level privacy preservation. We proposed the reverse k -NN labeling as a solution that limits every single record’s contribution, and is naturally immune to non-I.I.D. settings. After formulating the reverse k -NN labeling as bucketized sparse vector summation (BSVS), we provided concrete differentially private mechanisms under comprehensive scenarios (i.e., in centralized/local/shuffle settings). Theoretically, these mechanisms are guaranteed for labeling accuracy, which is determined by privacy budget and label count gaps. Experimentally, our solution achieved 99.1%/95.6% test accuracy (with $\epsilon = 0.1$) on the MNIST/SVHN dataset and 82.1% test accuracy (with $\epsilon = 1$) on the CIFAR-10 dataset, and improved significantly upon existing private knowledge-distillation/gradient-descent based methods with one magnitude lower of privacy consumption.

References

- Abadi, M.; Chu, A.; Goodfellow, I.; McMahan, H. B.; Mironov, I.; Talwar, K.; and Zhang, L. 2016. Deep learning with differential privacy. In *CCS*.
- An, S.; Lee, M.; Park, S.; Yang, H.; and So, J. 2020. An Ensemble of Simple Convolutional Neural Network Models for MNIST Digit Recognition. *arXiv preprint arXiv:2008.10400*.
- Berthelot, D.; Carlini, N.; Goodfellow, I.; Papernot, N.; Oliver, A.; and Raffel, C. A. 2019. Mixmatch: A holistic approach to semi-supervised learning. *Advances in Neural Information Processing Systems*, 32.
- Bittau, A.; Erlingsson, Ú.; Maniatis, P.; Mironov, I.; Raghunathan, A.; Lie, D.; Rudominer, M.; Kode, U.; Tinnes, J.; and Seefeld, B. 2017. Prochlo: Strong privacy for analytics in the crowd. In *SOSP*.
- Chang, A.; Ghazi, B.; Kumar, R.; and Manurangsi, P. 2021. Locally private k-means in one round. *ICML*.
- Chen, T.; Kornblith, S.; Norouzi, M.; and Hinton, G. 2020. A simple framework for contrastive learning of visual representations. *ICML*.
- Cheu, A.; Smith, A.; Ullman, J.; Zeber, D.; and Zhilyaev, M. 2019. Distributed differential privacy via shuffling. In *CRYPTO*.
- Dalal, N.; and Triggs, B. 2005. Histograms of oriented gradients for human detection. In *2005 IEEE computer society conference on computer vision and pattern recognition (CVPR'05)*, volume 1, 886–893. Ieee.
- Duchi, J. C.; Jordan, M. I.; and Wainwright, M. J. 2013. Local privacy and statistical minimax rates. *FOCS*.
- Dwork, C. 2006. Differential privacy. In *ICALP*. Springer.
- Feldman, V.; McMillan, A.; and Talwar, K. 2021. Hiding Among the Clones: A Simple and Nearly Optimal Analysis of Privacy Amplification by Shuffling. *FOCS*.
- Ghazi, B.; Kumar, R.; Manurangsi, P.; and Pagh, R. 2020. Private counting from anonymous messages: Near-optimal accuracy with vanishing communication overhead. In *ICML*.
- Hinton, G.; Vinyals, O.; and Dean, J. 2015. Distilling the knowledge in a neural network. *arXiv preprint arXiv:1503.02531*.
- Konečný, J.; McMahan, H. B.; Yu, F. X.; Richtárik, P.; Suresh, A. T.; and Bacon, D. 2016. Federated learning: Strategies for improving communication efficiency. *arXiv preprint arXiv:1610.05492*.
- Li, D.; and Wang, J. 2019. Fedmd: Heterogenous federated learning via model distillation. *arXiv preprint arXiv:1910.03581*.
- Lin, T.; Kong, L.; Stich, S. U.; and Jaggi, M. 2020. Ensemble distillation for robust model fusion in federated learning. *arXiv preprint arXiv:2006.07242*.
- Liu, R.; Cao, Y.; Chen, H.; Guo, R.; and Yoshikawa, M. 2020. Flame: Differentially private federated learning in the shuffle model. In *AAAI*.
- Luo, Y.; Zheng, L.; Guan, T.; Yu, J.; and Yang, Y. 2019. Taking a closer look at domain shift: Category-level adversaries for semantics consistent domain adaptation. In *CVPR*.
- Luo, Z.; Wu, D. J.; Adeli, E.; and Fei-Fei, L. 2021. Scalable Differential Privacy With Sparse Network Finetuning. In *CVPR*.
- Lyu, L.; and Chen, C.-H. 2020. Differentially private knowledge distillation for mobile analytics. In *SIGIR*.
- Monnier, T.; Groueix, T.; and Aubry, M. 2020. Deep Transformation-Invariant Clustering. In *NeurIPS*.
- Papernot, N.; Abadi, M.; Erlingsson, U.; Goodfellow, I.; and Talwar, K. 2016. Semi-supervised knowledge transfer for deep learning from private training data. *arXiv preprint arXiv:1610.05755*.
- Papernot, N.; Song, S.; Mironov, I.; Raghunathan, A.; Talwar, K.; and Erlingsson, Ú. 2018. Scalable private learning with pate. *ICLR*.
- Sun, L.; and Lyu, L. 2020. Federated model distillation with noise-free differential privacy. *arXiv preprint arXiv:2009.05537*.
- Van Gansbeke, W.; Vandenhende, S.; Georgoulis, S.; Proesmans, M.; and Van Gool, L. 2020. Scan: Learning to classify images without labels. In *ECCV*.
- Wang, J.; Bao, W.; Sun, L.; Zhu, X.; Cao, B.; and Philip, S. Y. 2019. Private model compression via knowledge distillation. In *AAAI*.
- Wang, S.; Li, J.; Qian, Y.; Du, J.; Lin, W.; and Yang, W. 2021. Hiding Numerical Vectors in Local Private and Shuffled Messages. *IJCAI*.
- Wei, K.; Li, J.; Ding, M.; Ma, C.; Yang, H. H.; Farokhi, F.; Jin, S.; Quek, T. Q.; and Poor, H. V. 2020. Federated learning with differential privacy: Algorithms and performance analysis. *IEEE Transactions on Information Forensics and Security*.
- Zhu, Y.; Yu, X.; Chandraker, M.; and Wang, Y.-X. 2020a. Private-knn: Practical differential privacy for computer vision. In *CVPR*.
- Zhu, Y.; Yu, X.; Tsai, Y.-H.; Pittaluga, F.; Faraki, M.; Wang, Y.-X.; et al. 2020b. Voting-based Approaches For Differentially Private Federated Learning. *arXiv preprint arXiv:2010.04851*.
- Zhu, Z.; Hong, J.; and Zhou, J. 2021. Data-Free Knowledge Distillation for Heterogeneous Federated Learning. *ICML*.

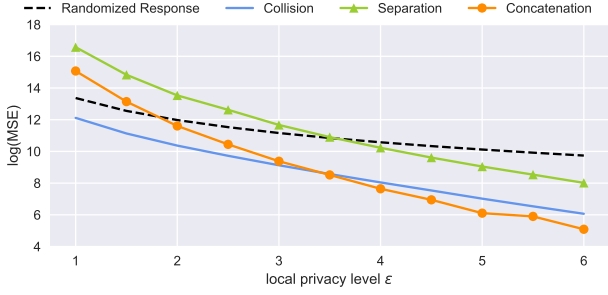


Figure 6: Comparison of local DP mechanisms in the low privacy regime for the BSVS problem with $n = 1$, $s = 200$, $|\mathcal{Y}| = 50$, $k = 2$, and $r = 2$.

APPENDIX

A. An Optimal Oracle for High Privacy

Due to budget splitting, the randomized response is suffering from the error rate of $\tilde{\Theta}(\frac{k \cdot r}{\epsilon})$. In this part, we adopt an optimal sparse vector summation oracle (in the high privacy regime) (Wang et al. 2021) for the BSVS problem and achieve an error rate of $\tilde{\Theta}(\frac{\sqrt{k \cdot r}}{\epsilon})$.

If we flatten the labeling answer A^i , essentially the BSVS problem is a special case of sparse vector summation where the domain size d is $s \cdot |\mathcal{Y}|$ and the maximum cardinality c is $k \cdot r$. One mean-squared-error optimal mechanism for sparse vector summation is the Collision mechanism (Wang et al. 2021) (see Definition 5), where all non-zero entries are mapped into a more dense Bloom filter with length l via local hashes.

Definition 5 ((d, c, ϵ, l) -Collision Mechanism (Wang et al. 2021)). Given a random-chosen hash function $H : \mathcal{G} \mapsto \mathcal{Z}$, take a vector V having c non-zero entries as the input ($V \subseteq \mathcal{G}$), the Collision mechanism randomly outputs an element $z \in \mathcal{Z}$ according to following probabilities:

$$\mathbb{P}[z|V] = \begin{cases} \frac{e^\epsilon}{\Omega}, & \text{if } \exists v \in V, z = H(v); \\ \frac{\Omega - e^\epsilon \cdot \#\{H(v) \mid H(v) \text{ for } v \in V\}}{(l - \#\{H(v) \mid H(v) \text{ for } v \in V\}) \cdot \Omega}, & \text{otherwise.} \end{cases} \quad (1)$$

The normalization factor is $\Omega = c \cdot e^\epsilon + l - c$. An unbiased estimator of indicator $\mathbb{1}[v \in V]$ (for $v \in \mathcal{G}$ when $c \geq 2$) is:

$$\mathbb{1}[v \in V] = \frac{\mathbb{1}[H(v) = z] - 1/l}{e^\epsilon/\Omega - 1/l}.$$

Setting the Bloom filter length l at around $2kr - 1 + kre^\epsilon$, we show that the Collision mechanism for the BSVS problem is $(O(\sqrt{\frac{nkr \log(|\mathcal{Y}|/\beta)}{\epsilon^2}}), \beta)$ -accurate (see Theorem 2).

Theorem 2. The $(s \cdot |\mathcal{Y}|, k \cdot r, \epsilon, 2k \cdot r - 1 + k \cdot r \cdot e^\epsilon)$ -Collision mechanism is an $(O(\sqrt{\frac{nkr \log(|\mathcal{Y}|/\beta)}{\epsilon^2}}), \beta)$ -accurate algorithm for the BSVS problem when $\epsilon = O(1)$.

Proof. Recall that the binary value $\mathbb{1}[H(v) = z]$ could be deemed as a Bernoulli variable with success rate of either $\frac{1}{l}$ or $\frac{e^\epsilon}{\Omega}$. Since the total count of observed ones is a summation of n independent Bernoulli variables, let u denote the estimation bias of one element in \tilde{a}_t , according to the multiplicative Chernoff bound and the fact that $\frac{e^\epsilon}{\Omega} \geq \frac{1}{l}$, we have

$\mathbb{P}[|u| > \eta \cdot n \cdot \frac{1}{e^\epsilon/\Omega - 1/l}] \leq \exp(\frac{-\eta^2 n}{2l})$. Therefore, when $l = 2k \cdot r - 1 + k \cdot r \cdot e^\epsilon$, with probability of $1 - \beta$, we have $|a_t - \tilde{a}_t|_{+\infty} \leq \frac{(k \cdot r \cdot e^\epsilon + 2k \cdot r - 1)(2k \cdot r \cdot e^\epsilon + k \cdot r - 1)}{k \cdot r \cdot (e^{2\epsilon} - 1) - (e^\epsilon - 1)} \sqrt{\frac{2n \log(|\mathcal{Y}|/\beta)}{l}}$. Applying $e^\epsilon \approx \epsilon + 1$, we have the bound. \square

B. An Improved Oracle for Low Privacy

In this part, we improve the accuracy of BSVS in the low privacy regime (e.g., when $\epsilon > 1$ with shuffling privacy amplification in the next section). Note that the labeling answer A^i of user i equals the multiplication of $T_i \in [0, 1]^{s \times 1}$ and $y_i \in [0, 1]^{1 \times |\mathcal{Y}|}$ (see detail in Definition 4). Instead of treating A^i as a flat vector, we could derive A^i from privately estimated T_i and y_i . There are two approaches to estimate T_i and y_i simultaneously:

- **Separation:** We evenly split the local budget into two parts, and estimate T_i and y_i separately. Using the sparse vector oracle of the Collision mechanism (Wang et al. 2021), the average mean squared error of each estimated entry \hat{a} in T_i (or \hat{b} in y_i) is then approximately $O(\frac{k}{\epsilon^2})$ (or $O(\frac{r}{\epsilon^2})$). Since most entries in T_i and y_i are zero (i.e., $\mathbb{E}[\hat{a}] = \mathbb{E}[\hat{b}] = 0$), for a multiplied entry $\hat{a} \cdot \hat{b}$ in A^i , we have its average mean squared error is approximately:

$$\text{Var}[\hat{a} \cdot \hat{b}] = \text{Var}[\hat{a}] \cdot \text{Var}[\hat{b}] = O(\frac{kr}{\epsilon^4}).$$

Compared to the approach in the previous subsection having error $O(\frac{kr}{\epsilon^2})$, when the privacy budget is relatively high, this approach is more accurate.

- **Concatenation:** We concatenate the T_i and y_i to compose a vector with length $s + |\mathcal{Y}|$ and $k + r$ non-zero entries. Utilizing the sparse vector oracle in previous subsections, we have the average mean squared error of each entry in T_i or y_i is then approximately $O(\frac{k+r}{\epsilon^2})$. Hence, for every multiplied entry in A^i , we have its average mean squared error is approximately $O(\frac{(k+r)^2}{\epsilon^4})$.

In Figure 6, we compare the mean squared error of $(s \cdot |\mathcal{Y}|, k \cdot r, \epsilon, 2k \cdot r - 1 + k \cdot r \cdot e^\epsilon)$ -collision mechanism with the Separation/Concatenation approaches. It is observed that the Concatenation approach is more accurate when privacy budget is high (e.g., when $\epsilon \geq 3.5$), and the Concatenation dominates the Separation in all cases (due to smaller constant factor in error bounds).

C. Beyond Reverse k -NN Connection

Recall that after privatization, the accuracy of a labeling answer a_t highly relies on the non-private count gap Gap_t between the true label and false labels. In order to increase the gap, it is desirable to assign more (similar) records to the t -th query. However, when utilizing the reverse k -NN rule for connecting records/queries, the degrees of queries might be imbalanced and some queries may only connect with few records, especially when domain shifts (Luo et al. 2019). Hence, we investigate more balanced connections.

Let a bi-partied graph $\mathcal{G} = (Q, D, E)$ denote the connection relation between queries Q and records D , where

$E \subseteq Q \times D$ is the set of edges/connections. Since the maximum degree of nodes in D is associated with privatization parameters, we here only consider connections $E \in \mathcal{E}^k$ that the nodes in D have the maximum degree of k . Let $sim(q, x) \in \mathbb{R}^+$ denote the similarity between a node $q \in Q$ and a node $x \in D$ (derived from the latent representation of q and x). Now for approximating the gap Gap_t , we define the score of a query q given connections E as:

$$Score(q) = \sum_{x \in D \text{ and } (q,x) \in E} sim(q, x).$$

The reverse k -NN rule is thus equivalent to maximizing the (arithmetic) mean of these scores: $\arg \max_{E \in \mathcal{E}^k} \frac{\sum_{q \in Q} Score(q)}{|Q|}$. Alternatively, we may seek for more balanced connections by maximizing the minimum: $\arg \max_{E \in \mathcal{E}^k} \min_{q \in Q} Score(q)$; or by maximizing the harmonic mean: $\arg \max_{E \in \mathcal{E}^k} \frac{|Q|}{\sum_{q \in Q} 1/Score(q)}$.